Detecting Wormholes in Friction Stir Welds from Welding Feedback Data

Enkhsaikhan Boldsaikhan
National Institute for
Aviation Research
Wichita State Univ.
Wichita, KS 67260
eboldsaikhan@niar.wichita.edu

Edward Corwin
Antonette Logar
Jeffrey McGough
Mathematics and CS
SDSM&T
Rapid City, SD 57701
edward.corwin@sdsmt.edu

William Arbegast
AMP Center
SDSM&T
Rapid City, SD 57701
william.arbegast@sdsmt.edu

ABSTRACT

This work describes a new non-destructive evaluation technique for detecting wormholes in friction stir welds. Feedback gathered during welding in both the time and frequency domains can be used to indicate the presence of a defect. Binned DFT frequencies of feedback signals were used as feature vectors for training a neural network. The approach was successful, recognizing 95% of novel inputs, but the network's ability to generalize is limited. Phase space analysis, a technique for comparing the signal to its time-derivative, provides a more robust option. Characterization of both the degree of circularity of the phase space diagram and the extent to which it is stationary has been tied to material flow and to defect formation. This technique was capable of detecting weld defects with 81% accuracy.

1. INTRODUCTION

Friction stir welding (FSW) is an innovative technique for joining metals that was developed and patented by The Welding Institute of Cambridge, England in 1991 [1]. In this work, a threaded probe with shoulder (pin tool) was rotated and plunged into the joint line between two workpieces forming a butt joint (Figure 1). Friction between the wear-resistant pin tool and material generates sufficient heat to plasticize the work pieces without melting. The rotation of the pin tool plays two important roles. First, it generates heat due to the friction, and second, it stirs the two plasticized work pieces together. As soon as the material reaches a plastic state, the rotating pin tool travels along the joint line and creates a solid-state bond between the two work pieces. While traveling along the joint line, the rotating pin tool has to have a downward forge load to maintain registered contact with the work pieces. Thus, three important parameters must be defined when making a weld : how fast the pin tool rotates, how fast the pin tool travels forward joining the two pieces, and how much force is exerted on the pin tool to maintain contact between the shoulder and the work pieces.

FSW has numerous advantages over fusion welding. It offers the ability to weld previously difficult or impossible combinations of materials, creates less distortion, allows for retention of parent material properties, requires lower energy consumption, produces diminished residual stresses, and is friendlier to the environment [2]-[5]. However, despite the simplified processing, an improper selection of system parameters may result in a weld with undesirable defects. One of the most common defects associated with FSW is a wormhole, a cavity completely below the weld surface undetectable to a human operator. The primary cause of a wormhole defect is abnormal material flow during welding. Because of the reduced joint area between the work pieces, wormholes severely weaken the mechanical properties of the weld bond. The research to date has concentrated on determining the presence of wormhole defects from feedback captured from the machine while the weld is being made. The final goal is a control algorithm that will adjust system parameters in real-time to prevent wormhole formation. Note that many factors may contribute to wormhole formation, such as clamping or pin tool geometry, but this study only varies the three parameters listed above, rotation speed, travel speed, and downward force, the thickness of the aluminum, and the alloy.

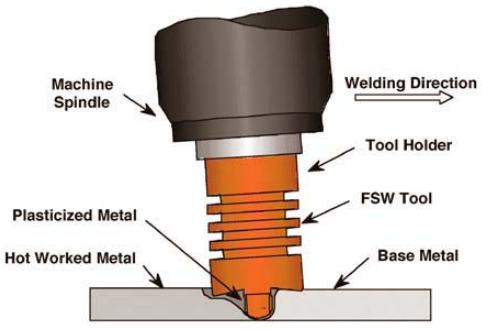

Figure 1: Drawing of a typical FSW pin tool

2. THE DATA

As noted above, an interesting problem in many FSW applications is how to determine the presence of wormholes. X-ray techniques have a high degree of accuracy, but the equipment needed to test the weld may not be available or feasible to use in all situations. This research provides an alternative technique in which feedback captured during the welding process is used for performing non-destructive evaluation of the weld quality.

The welding machine in use at the Center for Friction Stir Processing (CFSP) on the SDSM&T campus is an ISTIR-10 capable of recording a variety of feedback forces. The X feedback force is a measure of resistance to the weld in the direction of travel of the pin tool as a weld is being made, Z feedback force provides feedback on the force exerted in opposition to that of the downward pressure placed on the pin tool, and the Y feedback force measures the amount of sideways movement made during the weld. Note that welds can be made under position control or forge force control. In position control, the pin tool is placed at a particular height and remains at that fixed position. In forge force, a constant amount of downward pressure is maintained throughout the weld. Thus, greater variation would be expected in the Z feedback under position control than under forge force control. Correlation analysis indicates that the distribution of frequencies in the frequency spectra of the X, Y, and Z feedback forces are all indicators of weld quality to some degree, but the Y force appears to be the most strongly tied to the weld quality. Two approaches to using the feedback forces are described in this work : one uses the time domain feedback force data as captured by transducers on the weld head assembly of the pin tool, and the other uses the frequency spectra of these signals.

2.1 Time Domain Data

One of the obstacles to evaluating weld quality from the Y feedback, or any feedback parameter, is the presence of noise in the output signal. The welding process does not occur in an ideal environment but rather is influenced by external factors such as temperature, metallurgical variations, edge inconsistencies etc., as well as by the inevitable machine-specific variability. Investigations are on-going to identify and characterize all of the types of noise that contribute to the composition of the feedback signals, but, at present, only mechanical vibration noise is removed by a low-pass filter. The filter was implemented by computing the discrete Fourier transform (DFT) of the time series data, excising the high frequency components from the DFT, and computing the inverse DFT. High frequency components are defined to be those above the spindle frequency, where the spindle frequency index is found by :

index = spindle RPM / (60 * sampling rate (Hz) / number of points in DFT)

Figure 2(a) shows a sample of the original time series data (FSW06048-5) generated for a butt weld of two pieces of 0.25 inch thick aluminum 7075 welded at 8 ipm, with a pin

tool speed of 200 rpm, using forge force control and sampled at a rate of 68.2667 Hertz. Figure 2(b) presents the 256 point discrete Fourier transform of the original time series signal and indicates the spindle frequency for this sample, calculated from the equation above, to be at index 12.5 (rounded up 13) in the DFT array. Figure 2(c) shows the filtered time series data. The resulting signal is smoother, but more importantly, the trends in the data are more apparent once the high frequency noise is removed. The appropriateness of using a low pass filter for removing mechanical vibration noise during friction stir welding was noted in [4]. The resulting filtered time series data is used for the phase space analysis described briefly above and in more detail in a later section.

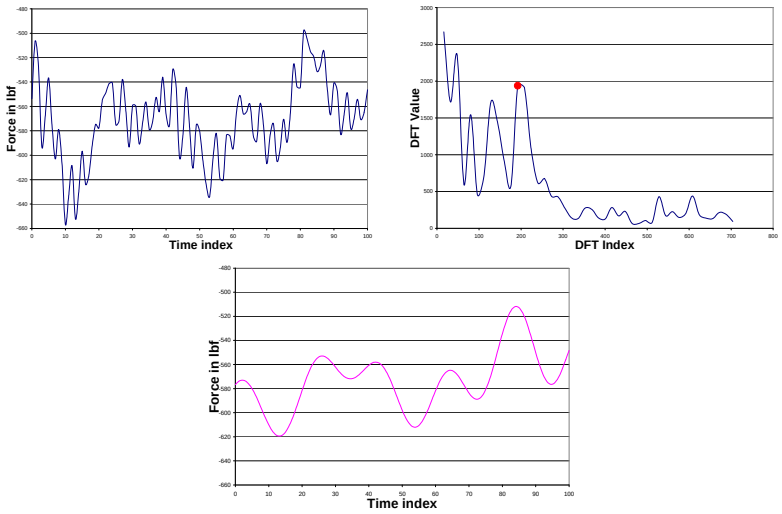

Figure 2: (a) Upper Left: the raw *y* force data. (b) Upper Right: the DFT for the data with the spindle frequency indicated (c) Bottom: the data after the low pass filter.

2.2 Frequency Domain Data

The neural network approach described below requires data to be transformed into feature vectors, compact representations of the data that retain the information necessary to group input vectors into classes. Often, large data sets can be segmented into small pieces and presented to the network for classification with little transformation. In this case, using small segments of the time domain data was not suitable as input to a neural network. Given the periodic nature of the welding process and the underlying material flow mechanics, frequency information is essential for recognizing patterns [6]-[11]. A discrete Fourier Transform was applied to the X, Y, and Z feedback forces for each set of feedback data, and the resulting frequency spectra were analyzed. Unstable material flow, the root cause of wormhole defects, appears to manifest itself in the frequency spectrum by an increase in low frequency components. Figure 3 depicts examples of the frequency spectra for a good (pictures a and b) and a bad (pictures d and e) weld generated from the X and Y feedback forces. Note that, as expected, the spindle frequency, the rate at which the pin tool is spinning, is the dominant frequency in a good weld. This indicates the material flow is being driven by the spindle. In the bad welds,

the spindle frequency is less clearly dominant, indicating other forces are strongly influencing the material flow. Also note that the magnitude of the low frequency components increases in the bad welds.

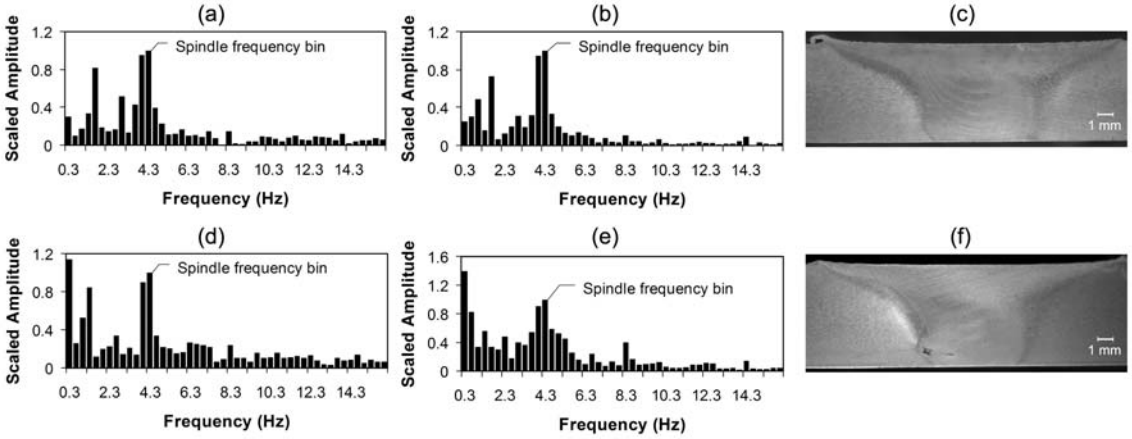

Figure 3: Representative examples of the manually identified frequency patterns of X force and Y force. The frequency pattern of X force in (a) and the frequency pattern of Y force in (b) correspond to a good weld, whose cross-sectional image is depicted in (c). Likewise, the frequency pattern of X force in (d) and the frequency pattern of Y force in (e) correspond to a bad weld, whose cross-sectional image with a wormhole defect is depicted in (f).

Since the low frequency portion of the spectrum provides the best differentiation, DFT values above the spindle frequency were ignored. Note that this is analogous to performing the low pass filter described in the time domain data section above. The remaining data was combined into bins by simply adding the DFT values within the bin. This provides a discrete approximation to summing the area under the curve for a continuous FFT (to within a scale factor). The optimal number of points per bin is not known, but given that smaller networks are faster and easier to train, the number of bins was restricted to 30 - 32 per feedback value to create manageable feature vectors. This approach proved effective for encapsulating the desired difference between data samples while creating input vectors small enough to allow for rapid training. A similar approach to generating feature vectors from the DFT was reported previously in [12] [13] when using a neural network for pattern classification based on ground penetrating radar.

The algorithm for generating the frequency domain feature vectors can be summarized as follows:

- Time domain feedback data was acquired from the machine during a weld.
- Appropriate sections of the weld were identified. Only the portions of the weld made when the process has reached steady-state are included.
- A 1024-point DFT was applied to the X and Y feedback forces for each weld. One set of feature vectors contained just Y values and a second set contained a combination of X and Y values.
- The spindle frequency is used to indicate the end of the useful data in the resulting DFT. Values above the spindle frequency are discarded.

- The resulting DFT data was partitioned into 30 or 32 bins by dividing the frequency spectrum into 32 equal length segments and assigning a value to each bin equal to the area under the curve for that segment of the frequency spectrum. The feature vector used for classification of a given sample is comprised of the 30-32 bin values.
- The vectors were labelled according to metallurgical quality.

A supervised-learning approach was selected for training the neural network which necessitated the creation of labeled samples, that is, feature vectors for which the correct classification (defect or no defect) is known to the network during training. These vectors are referred to as the training set. The testing set, consisting of novel samples not seen by the network during training, was used to test the network's ability to generalize within the parameters set for the experiment. It is important to note that all samples were taken from welds made on aluminum on the same machine using the same clamping, underlayment, and pin tool. Only the travel speed, rotation speed, alloy, and thickness of the material were varied. Thus, the results show the extent to which the network can generalize under these restrictions. Samples of good and bad welds are included in each data set as show in Tables 1 and 2.

	Good welds	Bad welds	Total Examples
Training set	46	8	54
Testing set	146	5	151
Total Examples	192	13	205

Table 1 : Number of vectors in the Training and the Testing Sets (Y feedback only)

	Good welds	Bad weld	Total Examples
Training set	84	96	180
Testing set	28	32	60
Total Examples	112	128	240

Table 2 : Number of vectors in the Training and the Testing Sets (X and Y feedback combined)

RPM = 425	IPM varied: 2, 4, 6, 7, 8, 10, 12
RPM = 500	IPM varied: 2, 4, 6, 7, 8, 10, 12
RPM = 350	IPM varied: 2, 4, 6, 7, 8, 10, 12
RPM = 450	IPM varied: 2, 7, 12, 7, 2
IPM = 7	RPM varied: 500, 425, 350, 300, 350, 425, 500

Table 3 : Weld Parameters (Y feedback only)

Travel Speed IPM	Spindle Speed RPM	Forge force lbs
25	300	11509
25	300	11809
25	300	12109
25	300	12409
20	300	11000
12	300	9600
3	300	6500
25	300	12609

Table 4 : Weld Parameters (X and Y feedback combined)

3. NEURAL NETWORK APPROACH

The application of a neural network to the problem of determining weld quality was first published in [8]. As a prelude to that study, a linear multiple regression analysis [14] was run on the training set using MiniTab software in order to see whether a linear relationship exists between the frequency patterns and the wormhole diameters. As a result, the R-squared value was about 35.8%, which means the governing relationship is most likely nonlinear. This suggests that a multilayer neural network would be an appropriate approach given the demonstrated capability of networks to construct nonlinear relationships between inputs and outputs.

As noted above, a supervised-learning approach was used which necessitated the creation of labeled samples, that is, feature vectors for which the correct classification (defect or no defect) is known to the network during training. These vectors are referred to as the training set. The testing set, consisting of novel samples not seen by the network during training, was used to test the network's ability to generalize within the parameters set for the experiment. It is important to note that all samples were taken from welds made on aluminum on the same machine using the same clamping, underlayment, and pin tool. Only the travel speed, rotation speed, alloy, and thickness of the material were varied. Thus, the results show the extent to which the network can generalize under these restrictions.

3.1 Network Topology and Training Parameters

The multilayer perceptron network, trained using the back propagation algorithm, that was implemented for this research is described in many sources [15]. A single perceptron, or node, receives one or many external inputs on weighted input lines,

computes the weighted sum of the inputs, and generates an output which is a function of that sum. The computed function, generally non-linear and continuous, produces a mapping from the input space to a classification space. Multilayer perceptron networks contain perceptrons arranged into an input layer, an output layer and one or two hidden layers (Fig. 4). Since arbitrary decision surfaces can be constructed with two hidden layers, more than two will not add functionality [16][17]. In this research, a single hidden layer proved sufficient.

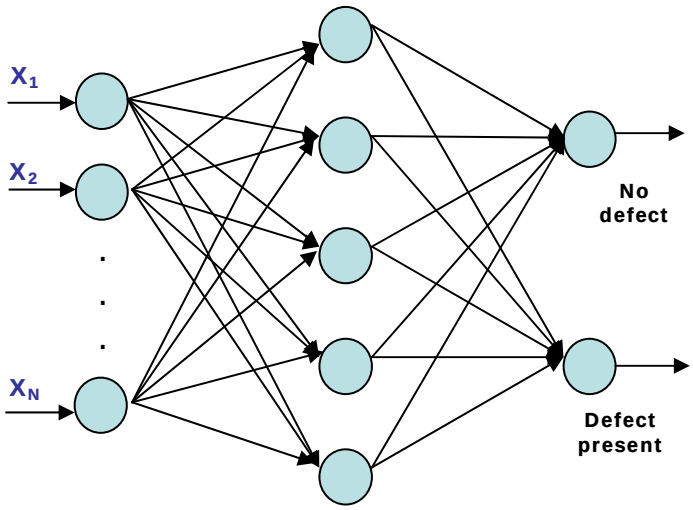

Figure 4: Sample neural network architecture. The networks used in these experiments consisted of 32 inputs plus a bias, 20 hidden nodes, and 2 output nodes for metallurgical quality.

The knowledge of the network is stored in the connection weights which are set to small random numbers between -0.1 and 0.1 when the network is initialized. During training, the error at a point in time is computed as the aggregate squared difference between the desired network outputs and the outputs actually produced by the weights at that time.

$$Error(t) = \frac{1}{2}\sum_i (Actual_i(t) - Desired_i(t))^2$$

The weights are adjusted using gradient descent to minimize that error. The technique relies on the computation of the partial derivative of the error with respect to each weight. A step size, often called the learning rate, is multiplied by the negative of the partial derivative, and this product is used to update of the weight:

$$\Delta w_{ij} = -\eta \frac{\partial E}{\partial w_{ij}}$$

The topology of the network used for assessing weld quality in the Y feedback only experiments had 32 inputs plus a bias, 20 hidden nodes, and 2 output nodes. If the first

output node responds to the input, the network classifies the weld as not containing a metallurgical defect; if the second output node responds, a defect is predicted to be present. Other system parameters necessary for reproducing these experiments are a learning rate of .1, the addition of a momentum term with a coefficient of .5, and 500 training iterations per experiment. Initial weights were set to random numbers in the range -0.1 to 0.1. The transfer function used at the hidden nodes and the output nodes was the sigmoid function:

$$f(x) = \frac{1}{1+e^{-x}}$$

Since neural network training can be sensitive to initial weights, four runs, each with different initial weights, were performed. The network was able to correctly classify all of the training and testing vectors, including vectors taken from welds with previously unseen rpm, ipm, material thickness, and alloys. However, in these initial experiments, all data was taken from position control welds. When forge force control data was used, network performance for Y values only dropped to 92%. Similar performance was observed when using vectors generated from the X feedback, but, interestingly, the types of errors were different. The network trained using the Y data set erred by not finding defects when they existed, but the analogous network trained with the X data set found more defects than actually existed. Thus, feature vectors were generated using the binned frequency spectra of both the X and Y feedback signals. For the first data set, when binning the Y feedback values, frequencies above the spindle frequency could be ignored. However, for the second data set, when using the X feedback in addition to Y, it was necessary to include frequencies up to twice the spindle frequency to achieve the desired accuracy. The resulting combined feature vectors had 96 elements which made training unacceptably slow. Frequency bins were pruned one at a time until the optimal vector size of 60 elements was determined. The resulting network was able to classify 98% of the training vectors and 95% of the testing vectors correctly and did not classify any defective welds as good (Table 5 and 6).

Additional experiments were conducted to determine the sensitivity of the network to other parameters. Experiments which sought to optimize the learning rate, momentum factor, the number of hidden units, and the number of output nodes – one or two outputs can be used for this problem – produced small improvements but none of significance. This demonstrates the robustness of the network; it was able to train to a high degree of accuracy with any reasonable set of starting conditions. Note that other conditions were held constant including the size of the initial weights and the number of epochs used for training. All results are the average of four runs as noted earlier.

Predicted Class vs. Actual Class	Category of good weld – Actual	Category of bad weld – Actual
Category of good weld – Predicted	81 / 84	0 / 96
Category of bad weld – Predicted	3 / 84	96 / 96

Table 5: Confusion Table for the Training Set

Predicted Class vs. Actual Class	Category of good weld – Actual	Category of bad weld – Actual
Category of good weld – Predicted	25 / 28	0 / 32
Category of bad weld – Predicted	3 / 28	32 / 32

Table 6: Confusion Table for the Testing Set

4. PHASE SPACE APPROACH

The neural network approach proved effective for determining weld quality and is useful in situations where welding conditions will not change, such as in industrial applications. However, the network's ability to generalize to different types of material or substantially different welding conditions is limited. A new network would need to be trained for each application. Another approach was developed which attempts to find a characterization of the feedback that is independent of the material or processing conditions. The motivation for this technique was found in dynamical systems[18][19]. Recall that the material flow in a good weld should be stable and periodic. From a dynamical systems perspective, this means that the changes that occur in the feedback forces should occur in a predictable or stable manner. Ideally, equations describing the system dynamics can be used for stability analysis, however, in many situations, those equations are not available or easily derived. In those cases, including this research, a sampling of the system outputs is used to approximate the system dynamics.

As noted above, the total magnitude of the low frequency components of the Y feedback values was strongly correlated to weld quality. This is the feedback force that quantifies the side-to-side motion experienced by the pin during welding, or more correctly, the variation in the motion of the pin tool perpendicular to the direction of the weld as it progresses through each rotation. Intuitively, this should also be the appropriate feedback for identifying aberrations in material flow since variations in material movement around the pin will manifest themselves in changes in the Y feedback force. Plotting the Y feedback values on the horizontal axis against the change in the Y values (Y') on the vertical axis provides a mechanism for examining the dynamics of the welding process with respect to the Y output value. As with position and velocity, the relationship between Y and Y' gives information about the behavior of the system. Also note that this behavior is abstracted from time and provides a compact framework within which the system dynamics can be examined and patterns easily recognized. These plots are commonly referred to as phase space diagrams or phase plots.

The curves formed by plotting a variable against its derivative through time are known as trajectories or orbits. In most physical systems, the trajectory will be bounded in some finite region of phase space and often tends to either a rest point or a limit cycle. A rest point is one where all system dynamics cease – the system is at rest. Limit cycles are

periodic solutions which attract or repel the orbits. After the transient behavior has died out, the flow is essentially on the limit cycle. In such cases, it is sensible to talk about the orbit as a closed curve since the trajectory will return to the same point and repeat the same sequence of values. Both fixed points and limit cycles are referred to as stable or unstable if they attract or repel the trajectories. As a simple example, plotting the function $f(t) = \sin(t)$ against its derivative $f'(t) = \cos(t)$ will produce a circle. No matter how large t becomes, the trajectory defined by plotting $f(t)$ vs. $f'(t)$ will always remain on the circle. This is an example of stable dynamics. Similarly, phase space plots indicated that the trajectories of the Y vs. Y′ plots tended to have stable orbits for good welds and tended to diverge from the orbits for bad welds. Examples of phase space plots of a good weld and a bad weld can be found in Figure 5. Figure 6 shows the location and size of the wormhole resulting from the bad weld in Figure 5. Note that the phase space plot of the spindle frequency (rpm) defines a stable orbit which can be considered to be the ideal trajectory for a weld made using the given system parameters. The spindle frequency orbit is plotted on the graphs to provide a reference for divergent or convergent behavior.

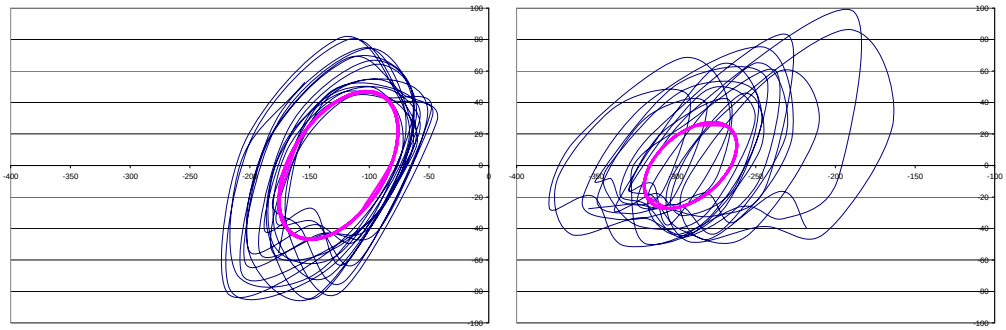

Figure 5: Phase space trajectory for the y force (horizontal axis) vs. the derivative of the y force (vertical axis) measured in foot-pounds (lbf). The phase space plot on the left is for a good weld, the plot on the right is for a bad weld. The trajectory of the spindle frequency is also plotted for reference.

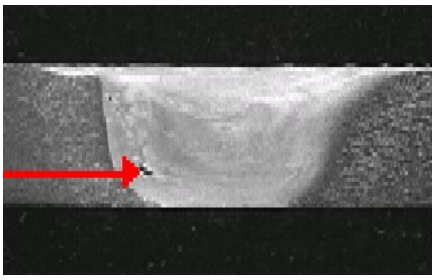

Figure 6: The location of the resulting wormhole at 40x magnification for the bad weld in Figure 5.

Visual inspection can easily distinguish very good welds from very bad welds as shown above. However, quantifying the degree of stability of a trajectory and determining a probability of defect based on the degree of divergence from the ideal has proved difficult. One approach that has produced reasonable results is the Poincaré Map [20]. In this approach, a hyperplane is positioned orthogonal to the direction of the trajectory. If

a trajectory is periodic and stable in its orbit, the trajectory will repeatedly cross the hyperplane at the same point. If the trajectory is nearly-periodic or has an orbit that returns to nearby points, the crossings will be tightly clustered. Note that the dynamics of the system are assumed to lie in a plane, an assumption which simplifies calculation but may lose valuable information about the trajectory. However, if the trajectory does remain in the plane, a reasonable hyperplane selection is the x-axis. Computing the standard deviation of the x values at each intersection of the trajectory with the x-axis provides a simple measure of stability. Table 7 gives the welding parameters used for butt joint welding of aluminum. From this data and the plot in Figure 7, a standard deviation of 1.0 will give perfect accuracy for identifying defects. Additional tests are needed to determine a general algorithm for setting the correct cutoff. Note that the weld made at 250 RPM and 10 inches per minute has no defects while the weld made at 250 and 16 inches per minute has a known wormhole. It is possible that the relatively high standard deviation for the 10 IPM weld indicates that the probability of making a wormhole is increasing as the pin tool is being pushed through the material at a faster rate. At 250 RPM the standard deviation is 0.12 at 2 IPM, 0.18 at 6 IPM, and jumps to 0.75 at 10 IPM. Thus, the standard deviation may prove useful for determining the limits of processing parameters for making defect-free welds.

RPM	IPM	Defect Size	SD
250	2	0	0.1200
425	6	0	0.1600
250	6	0	0.1800
425	10	0	0.1900
350	2	0	0.1900
350	6	0	0.2200
500	10	0	0.2400
500	2	0	0.2700
500	6	0	0.3400
350	10	0	0.3700
500	9	0	0.5000
250	10	0	0.7530
250	16	0.1000	1.0000
250	14	0.0500	1.0400
500	9	0.0600	1.1000

Table 7 : Welding parameters, observed defect area (mm^2), and standard deviation computed from the Poincaré Map of position control welds.

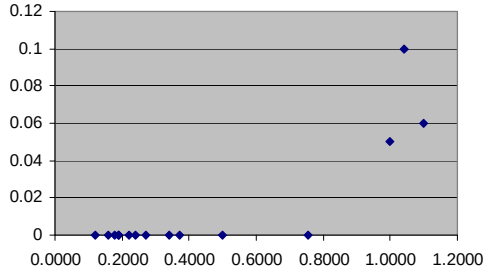

Figure 7: Standard deviation versus defect size. A cutoff of 1.0 produces accurate classification for position control welds. The horizontal axis is standard deviation and the vertical axis is the area of the wormhole (mm^2).

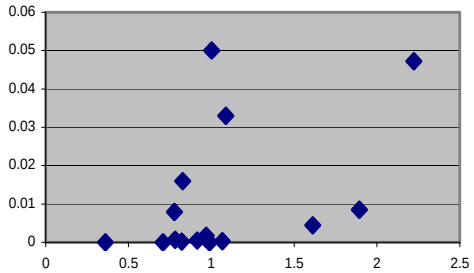

Figure 8: Standard deviation versus defect size. No cutoff produces accurate classification for forge force control. The horizontal axis is standard deviation and the vertical axis is the area of the wormhole (mm^2).

Unfortunately, the standard deviation method is only accurate for position control data. Forge force welds do not exhibit the same behavior (Fig. 8). For the experiments reported here, a standard deviation cutoff of 1.0 resulted in 81% accurate classification. From the chart it can be observed that it is possible for a good weld and a bad weld to have the same standard deviation under forge force control. Additional approaches are focusing on comparing the critical points of the expected trajectory with the actual trajectory and quantifying the degree and direction of divergence.

5. CONCLUSION

This work presents two approaches to non-destructive evaluation of weld quality in real-time. Other techniques require the completion of the weld before the presence or absence of defects can be determined making them unsuitable as a basis for a control algorithm. The DFT frequency spectra generated from feedback data obtained during the welding process can be binned and used as inputs to a previously trained neural network. When the welding parameters do not vary widely, this approach has resulted in perfect classification of both training and testing data. The more variation that can exist while making the weld, the less accurate the network becomes. Thus, for repetitive welding under similar conditions, the neural network has proven effective. If conditions change, a new network must be trained to generate new weights. The second approach removes this limitation by considering the stability of the feedback values. When the material flow around the pin tool is approximately the same with each revolution of the tool, the phase diagram of the feedback forces is stable – stationary and roughly circular. When the material flow fluctuates, one of the main causes of wormhole development, the phase diagram is not stable. In theory, this approach should be independent of the welding parameters since the flow of material around the pin tool must exhibit regular behavior to make a good weld under any conditions. This theory is currently being tested by varying the pin tool, the material, and the welding machine. Under position control, it has been possible to identify a cutoff value for the standard deviation of the Poincaré Map crossings that correctly classifies all welds. While this approach does not work as well for forge force welds, a technique which compares the critical points of the desired

trajectory with those of the actual weld shows great promise. Work is continuing on formulating a general approach to quantifying the stability of the trajectories and relating that value to weld quality.

References

[1] Thomas, W. M., Nicholas, E. D., Needham, J. C., Murch, M. G., Temple-Smith, P., and Dawes, C. J., Improvements relating to friction welding, TWI, EP 0 615 480 B1.

[2] Arbegast, W. J., Baker, K. S., and Hartley, P. J., "Fracture Toughness Evaluations of 2195 Al-Cu-Li Autogenous and Hybrid Friction Stir Welds," Proceedings of the 5th International Conference on Trends in Welding Research, Pine Mountain, GA, June 1-5, 1998, p. 558.

[3] Dracup, B., J., and Arbegast, W. J., "Friction Stir Welding as Rivet Replacement Technology," Proceedings of the 1999 SAE Aerospace Automated Fastening Conference & Exposition, Memphis, TN, October 5-7, 1999

[4] Li, Z. X., Arbegast, W. J., Wilson, A. L., Liu, J., and Hartley, P. J., "Post-Weld Aging of Friction Stir Welded 7249 Extrusions," Proceedings of the 6th International Conference on Trends in Welding Research, Pine Mountain, GA, April 15-19, 2002.

[5] Li, Z. X., Arbegast, W. J., and Hartley, P. J., "Microstructure Characterization and Stress Corrosion Evaluation of Friction Stir Welded AL 2195 and AL 2219 Alloys," Proceedings of the 5th International Conference on Trends in Welding Research, Pine Mountain, GA, June 1-5, 1998, p.568.

[6] Arbegast, W. J., "Using process forces as a statistical process control tool for friction stir welds," Friction Stir Welding and Processing III, Edited by K. V. Jata, M. W. Mahoney, R. S. Mishra, and T. J. Lienert, pp. 193-203, TMS, 2005.

[7] Morihara, T., Master of Science Graduate Thesis, South Dakota School of Mines and Technology, Rapid City, SD, USA, 2004.

[8] Boldsaikhan, E., Corwin, E. M., Logar, A. M., and W. J. Arbegast, "Neural network evaluation of weld quality using FSW feedback data," 6th Int. Friction Stir Welding Symposium, Montreal, Canada, 2006.

[9] Logar, A. M., Corwin, E. M., Boldsaikhan, E., Woodward, D., and Arbegast, W. J., "Applications of artificial intelligence to friction stir welding," National Conf. on Recent Advancements in Information Technology, Coimbatore, India, February 9-10, 2007.

[10] Jene, T., Dobmann, G., Wagner, G., and Eifler, D., "MonStir – Monitoring of the friction stir welding process," International Institute of Welding, Doc. III-1430-07.

[11] Fleming, P., et al., "In-process gap detection in friction stir welding," Sensor Review, vol. 28, no. 1, pp. 62-67, Emerald Group Publishing Limited, 2008.

[12] Weiss, J., Hartsel, C., Askildsen, B., and Thompson, S., "Artificial Neural Network-Based Human Target Detection Using Noninvasive Penetrating Radar Data", Proceedings

of the ISCA 19th International Conference on Computers and Their Applications, pp. 233-236, Mar 2004.

[13] Gervasi, A., Weiss, J., Askildsen, B., and Thompson, S., "Advances In Human Target Detection Using Opaque Material Penetrating Radar Data", Proceedings of the ISCA 20th International Conference on Computers and Their Applications, pp.202-207, Mar 2005.

[14] Montgomery, D. C., Design and Analysis of Experiments, 6th edition, John Wiley & Sons, Inc., 2005.

[15] Rumelhart, D., Hinton, G., and Williams, R., 1986, "Learning internal representations through error propagation", *Parallel Distributed Processing: Exploration in the Microstructure of Cognition*, edited by D. Rumelhart and J. McClelland, MIT Press, Cambridge, MA, 318-362.

[16] Blum, E. K. and Li, L. K., 1991, "Approximation theory and feedforward networks", *Neural Networks* 4 (4), 511-515.

[17] Jones, L. K., 1990, "Constructive approximations for neural networks by sigmoidal functions", *Proceedings of the IEEE* 78 (10), 1586-1589.

[18] Kantz, H., Schreiber, T., Nonlinear Time Series Analysis, 2nd edition, Cambridge University Press, 2003.

[19] Hirsch, M. W., Smale, S., and Devaney, R. L., Differential Equations, Dynamical Systems & Introduction to Chaos, 2nd edition, pp. 194-203, Elsevier (USA), 2004.

[20] Boldsaikhan, E., Corwin, E. M., Logar, A. M., McGough, J., and Arbegast, W. J., "Phase Space Analysis of Friction Stir Weld Quality," Friction Stir Welding and Processing IV, Edited by R.S. Mishra, et al, TMS, 2007.